The inhibition process of HIV-1 integrase by diketoacids molecules: Understanding the factors governing the better efficiency of dolutegravir

Léa El Khoury, Jean-Philip Piquemal, Serge Fermandjian, Richard G. Maroun, Nohad Gresh, Zeina Hobaika

The inhibition process of HIV-1 integrase by diketoacids molecules: understanding the factors governing the better efficiency of dolutegravir

Léa El Khoury[1,2*], Jean-Philip Piquemal[2,3,4], Serge Fermandjian[5], Richard G. Maroun[1], Nohad Gresh[2], and Zeina Hobaika[1*]

1 Centre d'Analyses et de Recherche, UR EGFEM, Faculté des Sciences, Université Saint-Joseph de Beyrouth, B.P. 11-514 Riad El Solh, Beirut 1107 2050, Lebanon

2 Laboratoire de Chimie Théorique, UMR7616 CNRS, UPMC, Sorbonne Universités, Paris 75005, France

3 Institut Universitaire de France, Paris Cedex 05, 75231, France

4 Department of Biomedical Engineering, the University of Texas at Austin, Austin, Texas 78712, United States

5 Chemistry and Biology Nucleo(S)Tides and Immunology for Therapy (CBNIT), UMR 8601 CNRS, UFR Biomédicale, Paris, France

E-mail addresses: lea.khoury4@net.usj.edu.lb, jpp@lct.jussieu.fr, sfermandjian@gmail.com, richard.maroun@usj.edu.lb, gresh@lct.jussieu.fr, and zeina.hobaika@usj.edu.lb

[*] Corresponding authors:

lea.khoury4@net.usj.edu.lb; Tel.: +961 1 42 10 00 Ext: 3468; Fax: +961 4 532657

zeina.hobaika@usj.edu.lb;   Tel.: +961 1 42 10 00 Ext: 3486; Fax: +961 4 532657

Abstract: The Human Immunodeficiency Virus-1 integrase is responsible for the covalent insertion of a newly synthesized double-stranded viral DNA into the host cells, and is an emerging target for antivirus drug design. Raltegravir (RAL) and elvitegravir (EVG) are the first two integrase strand transfer inhibitors used in therapy. However, treated patients eventually develop detrimental resistance mutations. By contrast, a recently approved drug, dolutegravir (DTG), presents a high barrier to resistance. This study aims to understand the increased efficiency of DTG upon focusing on its interaction properties with viral DNA. The results showed DTG to be involved in more extended interactions with viral DNA than EVG. Such interactions involve the halobenzene and scaffold of DTG and EVG and bases 5'G^{-4}3', 3'A^{3}5'and 3'C^{4}5'.

1. Introduction

Viral replication of Human Immunodeficiency Virus 1 (HIV-1)[1]depends mainly upon three viral enzymes: reverse transcriptase, protease and integrase [1, 2]. The catalytic functions of HIV-1 integrase (IN) are indispensable for the smooth integration process of the reverse-transcribed viral genome into host chromosome. This integration reaction follows two

Abbreviations: DKA, diketo acid; EVG, elvitegravir; HIV-1, Human Immunodeficiency Virus-1; IN, integrase; INSTIs, integrase strand transfer inhibitors; LTR, Long Terminal Repeats; MD, Molecular dynamics; NCI, Non-Covalent Interaction; PFV, Prototype Foamy Virus; RAL, raltegravir; ST, Strand transfer;

biochemical steps. The first, named 3'-processing, involves the cleavage of a GT dinucleotide downstream of a highly conserved CA dinucleotide at both 3'-ends of the viral DNA. The cleaved DNA is then inserted into the host genome by a direct transesterification reaction known as DNA strand transfer (ST) [3, 4]. Once integrated, the provirus persists in the host cell and serves as a template for the transcription of viral genes and replication of the viral genome, enabling the production of new viruses. IN thus represents a novel target for antiretroviral drug design, the more so, as it has no human counterpart. The first two US FDA approved integrase strand transfer inhibitors (INSTIs) were raltegravir (RAL) from Merck and Co [5, 6] and elvitegravir (EVG) from Japan Tobacco Inc. and Gilead Sciences [7-9]. Both are related to the diketo acid family (DKA), and inhibit the ST reaction by acting at the IN-DNA interface and are highly effective in reducing viral loads. EVG was shown to be a slightly more potent IN inhibitor than RAL [10-13]. RAL and EVG are administered as part of a multi-therapy treatment of AIDS since 2007 and 2012, respectively. However in the course of treatment, patients undergo viral resistance mutations that can severely limit the efficiency of these drugs [10-11, 14-16]. The latest DKA inhibitor, Dolutegravir (DTG) by Glaxo Smith Kline was introduced in the market in 2013. It is endowed with a much lesser sensitivity to emerging HIV-1 resistance mutations than the other INSTIs [17].

The X-ray structures of RAL, EVG and DTG complexed with the PFV (Prototype Foamy Virus) intasome, a viral PFV DNA-IN-Mg^{2+} complex, were solved by Hare et al. [7,18,19]. In addition to drug-protein and drug-metal interactions, all three structures showed the onset of extended drug-DNA interactions. These take place: a) between the inhibitor halogenated aromatic ring and the highly conserved 5'C^4A^3 3'/5'$T^{-3}G^{-4}$ 3' dinucleotide step; and b) between

the diketo ring and A^3 (shown in red at the 3'end of the oligonucleotides in Figure 1a), over which it is stacked.

Based on the X-ray structures, we have sought to unravel the contributions of individual viral DNA ends to inhibitor binding. A previous study led by our group [20] using spectroscopy had focused on the determinants of RAL affinity for these ends. Consistent with the X-ray analyses, it showed the RAL-processed viral DNA complex to be predominantly stabilized by the C^4, A^3 and G^{-4} bases (shown in red in Figure 1a). The present study compares EVG and DTG binding to viral DNA, correlating interaction affinities with their reported inhibitory properties [10]. To this aim, we have conducted fluorescence anisotropy experiments complemented by computational studies in the context of the Non Covalent Interaction (NCI) procedure [21]. We have considered the complexes of EVG and DTG with oligonucleotides mimicking processed (LTR32) and unprocessed (LTR34) viral DNA ends. Other oligonucleotide sequences derived from the U5 LTR (Long Terminal Repeats) extremity of viral DNA were also used in the fluorescence anisotropy titrations. All investigated LTR sequences are reported in Figure 1a. The purpose of this study is to put forth whether any increase in drug-DNA affinity correlates with a concomitant decrease of HIV-1 viral resistance mutation [20].

2. Materials and Methods

2.1. DNA samples and inhibitors

The oligonucleotides LTR34, LTR32, LTR32-I and LTR30 were purchased from Eurogentec (Belgium). The four LTRs of oligonucleotides were designed to adopt a folded double-stranded hairpin structure even under the low concentrations (10^{-9} to 10^{-5} M) used in fluorescence anisotropy experiments. The fluorescein reporter group is grafted on the central T

nucleotide (shown in green in Figure 1a) of the loop formed by the three thymine sequence (TTT). Folded LTR34 mimics the unprocessed U5 LTR end of viral DNA while LTR32 reproduces the 3'-processed viral DNA obtained by deletion of $5'G^2T^13'$ in the reactive strand after the highly conserved $5'C^4A^3 3'$ nucleotides (shown in red in the four oligonucleotides). LTR32-I (Inverted LTR-32) is a processed version of the viral DNA obtained by deletion of $5'A^{-1}C^{-2}3'$ (shown in blue in Figure 1a). The fourth oligonucleotide, LTR30, is a blunt-ended oligonucleotide lacking $5'G^2T^13':5'A^{-1}C^{-2}3'$. LTR32-I and LTR30 were used as controls to highlight the impact of the terminal dinucleotides during inhibition. EVG and DTG were purchased from AdooQ and Medchemexpress, respectively and their structures are represented in Figure 1b-c.

2.2. Fluorescence measurements

The thermodynamic parameters of the drug-DNA complexes were determined using fluorescence anisotropy on a Jobin-Yvon Fluoromax II instrument equipped with an Ozone-free 150 W xenon lamp. Fluorescence anisotropy was expressed as: $A = (I_{//} - I_{\perp})/ (I_{//} + 2I_{\perp})$ where parallel ($I_{//}$) and perpendicular ($I_{\perp}$) emission components were measured in L-format. The denominator of A was simply the total light that would be observed if no polarizers are used. With fluorescein as reporter, excitation was performed at 488 nm with a 4nm slit width. For LTR34 and LTR32, emission was recorded at 516 nm with a 5nm slit width while emission wavelengths were 515 and 514 nm, respectively, for LTR32-I and LTR30 with a slit width of 4 nm. During titrations, labeled DNA was dissolved to the desired concentration (8nM) in 800 µl phosphate buffer (10mM, pH 6, I=0.1) and placed in thermally jacketed quartz cells (1cm) controlled by a circulating bath at 5^oC; increasing concentrations of the inhibitors (EVG or DTG, respectively) were then added. The equilibrium dissociation constants (K_d) were determined by

5

fitting the sigmoidal curves, using the GraphPAD Prism 5 software which applies the non-linear regression (curve fit)-Least square procedure.

2.3. PDB entries

The high resolution cryo-EM structure of the HIV-1 intasome (PDB code: 5U1C) was recently resolved [21]. However, the structures of the HIV-1 intasome (IN-HIV-1 viral DNA-Mg^{2+}) in complex with RAL, EVG and DTG respectively have not been yet determined. Therefore, in the used computational approach, the complexes were extracted from the X-ray structures of the PFV intasome (IN-PFV viral DNA-Mg^{2+}) in complex with EVG [19] (PDB code: 3L2U) and DTG [20] (PDB code: 3S3M) respectively. PFV intasome crystal structures are generally used due to the lack of HIV intasome crystal structures and on account of structural and functional similarities of the two viruses.

2.4. NCI-Plot analyses

The weak interaction zones between the molecules were evaluated using quantum chemistry analyzing the electron density (promolecular) and its reduced gradient through the NCI (Non-Covalent Interaction) procedure with the NCI-Plot Program [22-23]. This procedure enables a visualization of the intermolecular interactions. The differentiation of the interaction depends on their nature and their strength (the density of the plots). The nature of the interaction can be differentiated by the color of the plot (blue= strong and attractive, green= weak interaction, red= strong and repulsive).

3. Results

3.1. Fluorescence studies

6

Fluorescence anisotropy is a well-adapted technique to evaluate and quantify ligand binding to DNA and proteins. It gives a non-disruptive means of measuring the association of a fluorescent ligand with another molecule [24] by providing insight on the stoichiometry and thermodynamic of the complex [25,26,27]. The binding isotherms illustrating the interaction of each fluorescein labeled oligonucleotide (LTR34, LTR32, LTR32-I, LTR30) with EVG and DTG are shown in Figures 2 and 3, respectively.

The titration curves of processed LTR32 with increasing concentrations of EVG (Figure 2a) and DTG (Figure 3a) are monophasic sigmoid and display important increases of anisotropy (about 0.8 units). However, although the increases of anisotropy are nearly the same, the Kd values are distinctly different: 0.95E-10 for EVG and 1.63E-12 for DTG, thus, translating a much stronger affinity for LTR32 in the case of DTG compared with EVG, for the same stoichiometry.

The binding of EVG and DTG to unprocessed LTR34 produces about the same increase of anisotropy (0.2 units), although smaller compared with processed LTR32. Here again, the Kd values (1.15 E-9 versus 2.0 E-11) attest to a higher affinity of DTG (10 folds) compared with EVG. In contrast, addition of EVG or DTG to inverted LTR32-I and blunt LTR (LTR30) does not produce any effect on anisotropy, proving that these drugs fail to interact with the extremities of the two modified oligonucleotides.

It is noteworthy that these results are consistent with clinical data reporting efficiencies of DTG and EVG [10], showing that the binding of drugs to DNA is the most important event during the IN inhibition process [20].

These experimental results highlight the key role of the flanking 5'A^{-1}C^{-2}3'dinucleotide in ultimate position of the uncleaved DNA strand (shown in blue in LTR32 of Figure 1) for the

binding of INSTIS to LTRs. This dinucleotide step may prevent the fraying of guanine G^{-4} on the facing reactive strand, retaining it in a, albeit distorted, stable H-bonded base pair with C^4. This arrangement will also enable G^{-4} to partake to interactions with the dihalogen ring of DTG/EVG. On another note, the 3'dinucleotide d (T^1G^2) on the unprocessed LTR34, limits the access of the drug to the terminal A^3 adenine. It also reduces the base fraying at A^3 contributing to an improved stacking with the DKA ring.

3.2. NCI-Plot analysis

Closely related recognition motives are highlighted by the crystal structures of the two PFV integrase-DKA inhibitor complexes [18, 19]. On the one hand, the halogenated aromatic rings stack under the processed viral DNA cytosine C^4, and simultaneously bind to guanine G^{-4} on the opposite strand. Binding to G^{-4} is driven by the interaction of the sigma hole prolonging the CF bonds with the electron-rich rings of G^{-4}. On the other hand, the diketo ring stacks over A^3.

Analyses of the intermolecular interaction energies of a series of halogenated derivatives with the G^{-4}-C^4 base pair were recently reported by us by parallel ab initio quantum chemistry and polarizable molecular mechanics calculations [26, 27]. As a complement to these studies, we perform here a topological analysis of the binding of the entirety of both EVG and DTG with an extended recognition zone encompassing G^{-4}, C^4 and A^3. This was done in the context of the NCI procedure as implemented in the NCI-Plot program [22]. The results reflect important interactions (electrostatic and van der Waals) of each INSTI with the processed viral DNA ends (Figure 4) with DTG scoring the best interaction plot (Figure 4b). A quantitative evaluation is given in Supplementary data (Figure S.1).

The interaction plots showed in Figure 4 highlight the fact that the intercalation of the drug between the two viral DNA strands is not only guided by the halobenzene ring but also by the rest of the ligand. In fact, intense, large and green plots are recorded in the whole pocket formed by C^4A^3-G^{-4} and either EVG or DTG. These reveal strong non-covalent interactions within the drug-DNA complex. In addition, the green plot represented in Figure 4b for the DTG complex has broader extensions than the one corresponding to the EVG complex (Figure 4a). Such a finding is consistent with those from fluorescence anisotropy and suggests a possible reason behind the better efficiency of DTG in clinical trials [10]. The affinities of the drug entities for the G^{-4}/C^4A^3 pocket may be impacted by their electron densities and can be subtly tuned by the nature and the position of their substituents. A more detailed computational work assessing the impact of such interactions will be given in a forthcoming paper [El Khoury et. al, in preparation].

4. Discussion

Both EVG and DTG are novel DKA derivatives affecting HIV-1 replication by inhibiting IN-mediated ST. While the first two marketed IN inhibitors, RAL and EVG, display a remarkable efficiency for HIV-1 patients, they induce important resistance mutations in the enzyme. Such mutations are less prone to occur with DTG. A previous paper had shown that the viral DNA, not the protein, is the primary target of RAL [20]. As a follow-up, we focused in this short communication on EVG and DTG, both of which are more effective than RAL. We addressed the following point: if the inhibitory effect of antiretroviral drugs is indeed exerted at the level of the viral LRT ends, do their binding affinities for such ends parallel the corresponding differences of their inhibitions of IN-mediated ST?

The experimental results showed that whether the LTR is processed or unprocessed, DTG is always endowed with a greater affinity than EVG. Despite their important structural differences, EVG and DTG dock in a similar manner in a well-defined pocket at the viral DNA end. This binding site is of high therapeutic interest since it is crucial for the viral DNA interactions with IN [30, 31]. Thus, targeting this site reinforces the inhibition of the integration mechanism [32]. NCI-plots highlight the match between the C^4-G^{-4} base pair and the halobenzene ring on the one hand, and between A^3 and the DKA ring on the other hand. More favorable overlaps are quantified in the case of DTG than EVG, which could contribute to the enhanced affinity of DTG.

Both INSTI complexes are more stable in the processed than in the unprocessed site. Thus, the fluorescence anisotropy results indicated the main involvement of the 5'$A^{-1}C^{-2}$3' dinucleotide in the binding of DKA(s). These findings are in agreement with previous data describing HIV-1 viral DNA as a main target of the first designed DKA inhibitors, highlighting the importance of $d(A^{-1}C^{-2})$ in the recognition mechanism required for strand transfer inhibition [7, 20, 28, 33-35].

There appear to be stringent requirements concerning the sequence of the nucleic bases at the ends of the LTR for retroviral integration [35-40], and there is no evidence of mutations in the LTRs that could lead to resistance to INSTIs. The design of new-generation inhibitors should then benefit from the conservative nature of the base sequence at the viral ends. More specific antiviral compounds, less prone to induce resistance mutations, could be tailored by increasing the number of interactions with processed viral DNA rather than with the protein. Following this preliminary study, the PFV intasome has been constructed with AMOEBA polarizable force field and is being currently equilibrated prior to molecular dynamics (MD) simulations. These will be performed on the respective intasome-inhibitor (RAL/EVG/DTG) complexes [EL

10

Khoury et al., to be published], using a massively parallel version of TINKER, TINKER-HP

[41]. We believe that MD simulations will further clarify the role of 5'A^{-1}C^{-2}3' dinucleotide on

preventing G^{-4} fraying. Furthermore, the role of other nucleotides in the LTR can better be

demonstrated and supported by such simulations.

References

[1]   Y. Pommier, A.A. Johnson, C. Marchand, Integrase inhibitors to treat HIV/AIDS, Nat. Rev. Drug Discov. 4 (2005) 236-248.

[2]   C.S. Adamson, E.O. Freed, Human immunodeficiency virus type 1 assembly, release, and maturation, Adv. Pharmacol.55 (2007) 347-387.

[3]   X. Li, L. Krishnan, P. Cherepanov, A. Engelman, Structural biology of retroviral DNA integration, Virology. 411 (2011) 194-205.

[4]   J.A. Grobler, K. Stillmock, B. Hu, M. Witmer, P. Felock, A.S. Espeseth, A. Wolfe, M. Egbertson, M. Bourgeois, J. Melamed, Diketo acid inhibitor mechanism and HIV-1 integrase: implications for metal binding in the active site of phosphotransferase enzymes, Proc. Natl. Acad. Sci. U.S.A. 99 (2002) 6661-6666.

[5]   B. Grinsztejn, B.-Y. Nguyen, C. Katlama, J.M. Gatell, A. Lazzarin, D. Vittecoq, C.J. Gonzalez, J. Chen, C.M. Harvey, R.D. Isaacs, Safety and efficacy of the HIV-1 integrase inhibitor raltegravir (MK-0518) in treatment-experienced patients with multidrug-resistant virus: a phase II randomised controlled trial, Lancet. 369 (2007) 1261-1269.

[6]   K.K. Koelsch, D.A. Cooper, Integrase inhibitors in salvage therapy regimens for HIV-1 infection, Curr. Opin. HIV and AIDS. 4 (2009) 518-523.

[7]   S. Hare, S.S. Gupta, E. Valkov, A. Engelman, P. Cherepanov, Retroviral intasome assembly and inhibition of DNA strand transfer, Nature. 464 (2010) 232-236.

[8]   M. Sato, T. Motomura, H. Aramaki, T. Matsuda, M. Yamashita, Y. Ito, H. Kawakami, Y. Matsuzaki, W. Watanabe, K. Yamataka, Novel HIV-1 integrase inhibitors derived from quinolone antibiotics, J. Med. Chem. 49 (2006) 1506-1508.

[9]   D. Da Silva, L. Van Wesenbeeck, D. Breilh, S. Reigadas, G. Anies, K. Van Baelen, P. Morlat, D. Neau, M. Dupon, L. Wittkop, HIV-1 resistance patterns to integrase inhibitors in antiretroviral-experienced patients with virological failure on raltegravir-containing regimens, J. Antimicrob. Chemother. 65 (2010) 1262-1269.

[10]   M. Métifiot, C. Marchand, K. Maddali, Y. Pommier, Resistance to integrase inhibitors, Viruses. 2 (2010) 1347-1366.

[11]   J. Marinello, C. Marchand, B.T. Mott, A. Bain, C.J. Thomas, Y. Pommier, Comparison of Raltegravir and Elvitegravir on HIV-1 Integrase Catalytic Reactions and on a Series of Drug-Resistant Integrase Mutants, Biochemistry. 47 (2008) 9345-9354.

[12]   M. Métifiot, K. Maddali, A. Naumova, X. Zhang, C. Marchand, Y. Pommier, Biochemical and pharmacological analyses of HIV-1 integrase flexible loop mutants resistant to raltegravir, Biochemistry. 49 (2010) 3715-3722.

[13]   M. Métifiot, N. Vandegraaff, K. Maddali, A. Naumova, X. Zhang, D. Rhodes, C. Marchand, Y. Pommier, Elvitegravir overcomes resistance to raltegravir induced by integrase mutation Y143, Aids. 25 (2011) 1175-1178.

[14]   D.J. Hazuda, P. Felock, M. Witmer, A. Wolfe, K. Stillmock, J.A. Grobler, A. Espeseth, L. Gabryelski, W. Schleif, C. Blau, Inhibitors of strand transfer that prevent integration and inhibit HIV-1 replication in cells, Science. 287 (2000) 646-650.

[15]   S. Reigadas, G. Anies, B. Masquelier, C. Calmels, L.J. Stuyver, V. Parissi, H. Fleury, M.-L. Andreola, The HIV-1 integrase mutations Y143C/R are an alternative pathway for resistance to Raltegravir and impact the enzyme functions, PLoS ONE. 5 (2010) e10311.

[16]   L. Wittkop, D. Breilh, D. Da Silva, P. Duffau, P. Mercié, I. Raymond, G. Anies, H. Fleury, M.-C. Saux, F. Dabis, Virological and immunological response in HIV-1-infected patients with multiple treatment failures receiving raltegravir and optimized background therapy, ANRS CO3 Aquitaine Cohort, J. Antimicrob. Chemother. 63 (2009) 1251-1255.

[17]   L. Vandekerckhove, GSK-1349572, a novel integrase inhibitor for the treatment of HIV infection, Curr. Opin. Investig. Drugs. 11 (2010) 203-212.

[18]   S. Hare, A.M. Vos, R.F. Clayton, J.W. Thuring, M.D. Cummings, P. Cherepanov, Molecular mechanisms of retroviral integrase inhibition and the evolution of viral resistance, Proc. Natl. Acad. Sci. U.S.A. 107 (2010) 20057-20062.

[19]   S. Hare, S.J. Smith, M. Métifiot, A. Jaxa-Chamiec, Y. Pommier, S.H. Hughes, P. Cherepanov, Structural and functional analyses of the second-generation integrase strand transfer inhibitor dolutegravir (S/GSK1349572), Mol. Pharmacol. 80 (2011) 565-572.

[20]   F.F. Ammar, S. Abdel-Azeim, L. Zargarian, Z. Hobaika, R.G. Maroun, S. Fermandjian, Unprocessed viral DNA could be the primary target of the HIV-1 integrase inhibitor raltegravir, PloS ONE. 7 (2012) e40223.

[21]   D.O. Passos, M. Li, R. Yang, S.V. Rebensburg, R. Ghirlando, Y. Jeon, N. Shkriabai, M. Kvaratskhelia, R. Craigie, D. Lyumkis, Cryo-EM structures and atomic model of the HIV-1 strand transfer complex intasome, Science. 355 (2017) 89-92.

[22]   E.R. Johnson, S. Keinan, P. Mori-Sanchez, J. Contreras-Garcia, A.J. Cohen, W. Yang, Revealing noncovalent interactions, J. Am. Chem. Soc. 132 (2010) 6498-6506.

[23]   J. Contreras-García, E.R. Johnson, S. Keinan, R. Chaudret, J.-P. Piquemal, D.N. Beratan, W. Yang, NCIPLOT: a program for plotting noncovalent interaction regions, J. Chem. Theory Comput. 7 (2011) 625-632.

[24]   A.M. Rossi, C.W. Taylor, Analysis of protein-ligand interactions by fluorescence polarization, Nat. Protoc. 6 (2011) 365-387.

[25]   T. Heyduk, J.C. Lee, Application of fluorescence energy transfer and polarization to monitor Escherichia coli cAMP receptor protein and lac promoter interaction, Proc. Natl. Acad. Sci. U.S.A. 87 (1990) 1744-1748.

[26]   J.J. Hill, C.A. Royer, Fluorescence approaches to study of protein-nucleic acid complexation, Methods Enzymol. 278 (1997) 390-416.

[27]   L. Zargarian, M.S. Benleumi, J.-G. Renisio, H. Merad, R.G. Maroun, F. Wieber, O. Mauffret, H. Porumb, F. Troalen, S. Fermandjian, Strategy to discriminate between high and low affinity bindings of human immunodeficiency virus, type 1 integrase to viral DNA, J. Biol. Chem. 278 (2003) 19966-19973.

[28]   K. El Hage, J.-P. Piquemal, Z. Hobaika, R.G. Maroun, N. Gresh, Substituent-modulated affinities of halobenzene derivatives to the HIV-1 integrase recognition site. Analyses of the interaction energies by parallel quantum chemical and polarizable molecular mechanics, J. Phys. Chem. A. 118 (2014) 9772-9782.

[29]   K. El Hage, J.P. Piquemal, Z. Hobaika, R.G. Maroun, N. Gresh, Could the "Janus-like" properties of the halobenzene CX bond (X, Cl, Br) be leveraged to enhance molecular recognition?, J. Comput. Chem. 36 (2015) 210-221.

[30]   Z. Hobaika, L. Zargarian, Y. Boulard, R.G. Maroun, O. Mauffret, S. Fermandjian, Specificity of LTR DNA recognition by a peptide mimicking the HIV-1 integrase α4 helix, Nucleic Acids Res. 37 (2009) 7691-7700.

[31]   Z. Hobaika, L. Zargarian, R. Maroun, O. Mauffret, T. Burke Jr, S. Fermandjian, HIV-1 integrase and virus and cell DNAs: complex formation and perturbation by inhibitors of integration, Neurochem. Res. 35 (2010) 888-893.

[32]   M. Métifiot, B.C. Johnson, E. Kiselev, L. Marler, X.Z. Zhao, T.R. Burke, C. Marchand, S.H. Hughes, Y. Pommier, Selectivity for strand-transfer over 3′-processing and susceptibility to clinical resistance of HIV-1 integrase inhibitors are driven by key enzyme–DNA interactions in the active site, Nucleic Acids Res. (2016) gkw592.

[33]   S. Hare, G.N. Maertens, P. Cherepanov, 3′-Processing and strand transfer catalysed by retroviral integrase in crystallo, EMBO J. 31 (2012) 3020-3028.

[34]   F.F. Ammar, Z. Hobaika, S. Abdel-Azeim, L. Zargarian, R.G. Maroun, S. Fermandjian, A targeted DNA substrate mechanism for the inhibition of HIV-1 integrase by inhibitors with antiretroviral activity, FEBS Open Bio. (2016).

[35]   A. Caumont, G. Jamieson, V.R. de Soultrait, V. Parissi, M. Fournier, O.D. Zakharova, R. Bayandin, S. Litvak, L. Tarrago-Litvak, G.A. Nevinsky, High affinity interaction of HIV-1 integrase with specific and non-specific single-stranded short oligonucleotides, FEBS lett. 455 (1999) 154-158.

[36]   R.L. LaFemina, P. Callahan, M.G. Cordingley, Substrate specificity of recombinant human immunodeficiency virus integrase protein, J. Virol. 65 (1991) 5624-5630.

[37]   C. Vink, D. Van Gent, Y. Elgersma, R. Plasterk, Human immunodeficiency virus integrase protein requires a subterminal position of its viral DNA recognition sequence for efficient cleavage, J. Virol. 65 (1991) 4636-4644.

[38]   R. Craigie, T. Fujiwara, F. Bushman, The IN protein of Moloney murine leukemia virus processes the viral DNA ends and accomplishes their integration in vitro, Cell. 62 (1990) 829-837.

[39]   F.D. Bushman, R. Craigie, Activities of human immunodeficiency virus (HIV) integration protein in vitro: specific cleavage and integration of HIV DNA, Proc. Natl. Acad. Sci. U.S.A. 88 (1991) 1339-1343.

[40]   P.A. Sherman, M.L. Dickson, J.A. Fyfe, Human immunodeficiency virus type 1 integration protein: DNA sequence requirements for cleaving and joining reactions, J. Virol. 66 (1992) 3593-3601.

[41]   F.L. L. Lagardère, B. Stamm, E. Polack, L. H. Jolly, C. Narth, E. Kratz, G. A. Cisneros, M. Schnieders, T. A. Darden, N. Gresh, Y. Maday, J. W. Ponder, P. Y. Ren, J. P. Piquemal UPMC, Tinker-HP, Version 1.0, UPMC, Sorbonne Universités, Paris, 2016
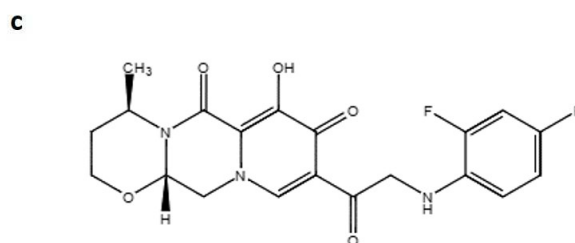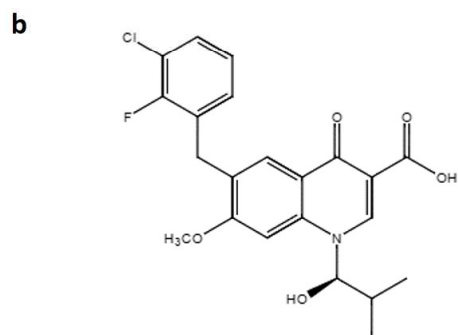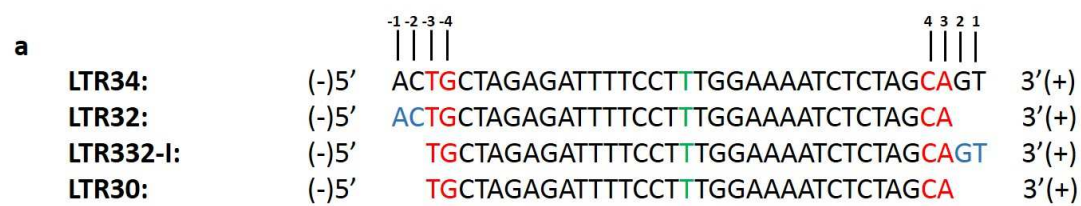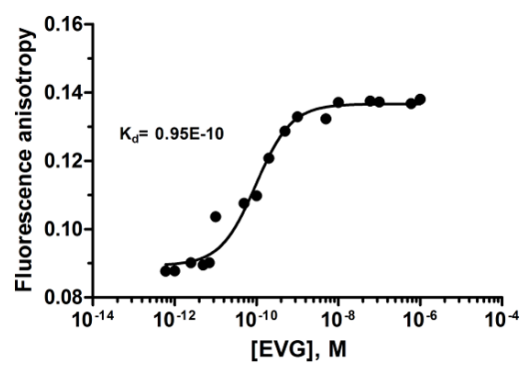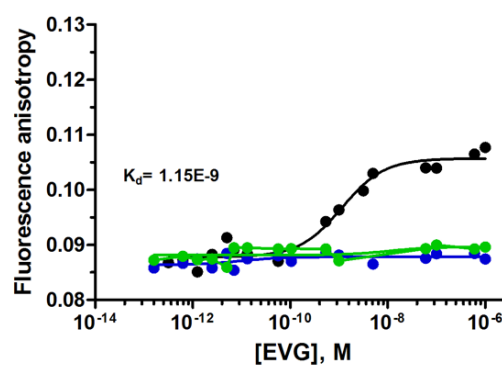
Figure legends

Figure 1. a) the four oligonucleotides with the central three thymines (TTT) enabling their folding into hairpin (loop-stem) structures; b) elvitegravir; and c) dolutegravir.
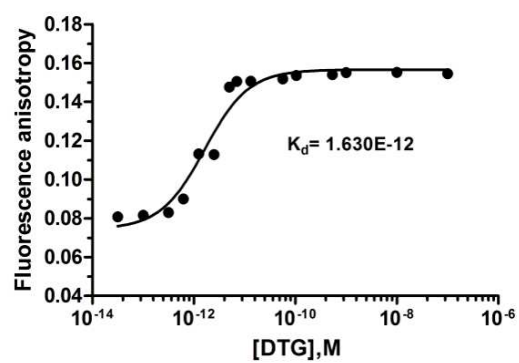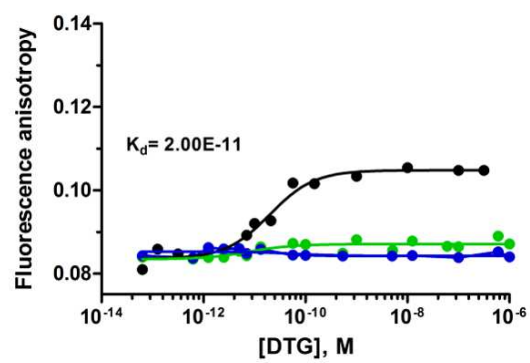
Figure 2. Fluorescence anisotropy analysis of elvitegravir binding to oligonucleotides. 2a. Titration curve of LTR32. **2b.** Titration curves of LTR34 (black), LTR32-I (green) and LTR30 (blue) at 8 nM by increasing concentrations of EVG (from 10^{-13} to 10^{-6}). Values of K_d yielded by treatment of the EVG-LTR32 and EVG-LTR34 titration curves are inserted on the graphs.
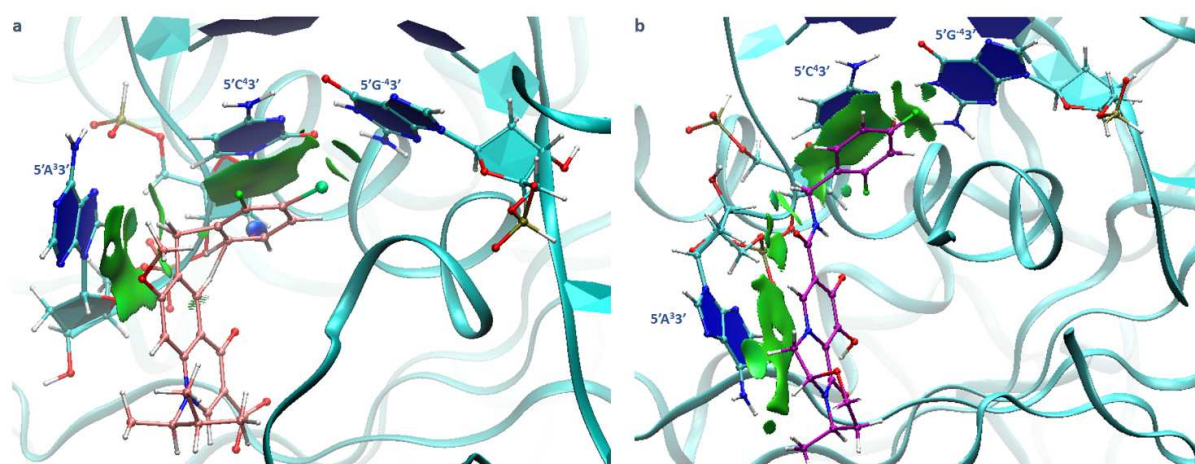
Figure 3. Fluorescence anisotropy analysis of dolutegravir binding to oligonucleotides. 3a. Titration curve of LTR32. **3b.** Titration curves of LTR34 (black), LTR32-I (green) and LTR30 (blue) at 8 nM by increasing concentrations of DTG (from 10^{-13} to 10^{-6}). Values of K_d yielded by treatment of the DTG-LTR32 and DTG-LTR34 titration curves are inserted on the graphs.

Figure 4. Representation of the IN−DNA-DKA complex focusing on: **a.** The recognition site of the elvitegravir halobenzene and scaffold in interaction with G^{-4}, C^4 and A^3 bases at the viral DNA ends. EVG is shown in pink and the green plots are the respective intermolecular interaction surfaces. **b.** The recognition site of the dolutegravir halobenzene and scaffold in interaction with G^{-4}, C^4 and A^3 bases at the viral DNA ends. DTG is shown in purple and the green plots are the respective intermolecular interaction surfaces. All interactions were generated by the NCI-plot procedure.

a


```
                              -1 -2 -3 -4                                    4 3 2 1
                               | | | |                                       | | | |
LTR34:      (-)5'    ACTGCTAGAGATTTTCCTTTGGAAAATCTCTAGCAGT    3'(+)
LTR32:      (-)5'    ACTGCTAGAGATTTTCCTTTGGAAAATCTCTAGCA      3'(+)
LTR332-I:   (-)5'      TGCTAGAGATTTTCCTTTGGAAAATCTCTAGCAGT    3'(+)
LTR30:      (-)5'      TGCTAGAGATTTTCCTTTGGAAAATCTCTAGCA      3'(+)
```

b

c

a

K_d= 0.95E-10

Fluorescence anisotropy

[EVG], M

b

K_d= 1.15E-9

Fluorescence anisotropy

[EVG], M

a

b

Highlights

- Elvitegravir and Dolutegravir demonstrate high affinities towards HIV viral DNA
- Dolutegravir displays the most specific interactions with HIV viral DNA extremities
- Increase in drug-DNA affinity correlates with decrease of HIV resistance mutation
- Dolutegravir derivatives could be promising potent HIV inhibitors
- Experimental/Computational Approach elucidating the HIV integrase inhibition